

<https://doi.org/10.32056/KOMAG2021.4.3>

## Strength analysis for cycloidal gears with the new concept of power transmissions

Received: 19.10.2021

Accepted: 07.12.2021

Published online: 29.12.2021

### Author affiliation and address:

Wrocław University of Science and  
Technology, Ignacego Łukasiewicza  
7/209a, 50-371 Wrocław, Poland

### Correspondence:

e-mail: [krzysztof.biernacki@pwr.edu.pl](mailto:krzysztof.biernacki@pwr.edu.pl)

Krzysztof BIERNACKI 

### Abstract:

The article presents a new design solution of hydraulic gerotor machines. The main attention was paid to the analysis of strain behaviour of a cycloidal gear set. The gears are the main assemblies of hydraulic gerotor machines, which are powered by driving the gear set. In the state of the art, the rotational motion of the gear set was effected by driving the inner gear. This article proposes a modified method of power transmission in which the outer gear is now a driving gear. Such a solution also results in modifications to the hydraulic machine design. This has led to a concept of a new hydraulic gerotor machine, which differs from the traditional designs. The device according to the new design is capable of carrying substantially higher loads than devices of the previous designs.

Keywords: strength analysis, plastics, Finite Elements Method (FEM), conceptual designing



## 1. Introduction

Hydraulic machines and hydraulic equipment have been used from the very beginning of human industrial activity. The first to appear were piston pumps used in maritime transport and railways [1]. Gear machines of more advanced design appeared later. Hydraulic gear machines are divided into the following three types:

- gear machines with external meshing,
- gear machines with internal meshing,
- gerotor machines.

The gerotor machines appeared at the latest. Their mass production was started by the Henry Nichols company in the USA in the 1930s in the USA.

Gerotor machines are of an innovative design solution and have many utility advantages. They have a simple structure, small dimensions and weight, high efficiency and low pulsation of this efficiency. A set of gears with internal cycloidal meshing is the key group of gerotor pumps.

Typical hydraulic gerotor machine is presented in Fig. 1.

The main working unit of this machine consists of two cycloidal wheels, which are the idler wheel (1) and the driving wheel (2). They are wheels with internal meshing. The idler wheel, in this assembly, has a greater number of teeth than the driving wheel. The difference in the number of teeth is always  $z_2 - z_1 = 1$ . The figures (Fig. 1, Fig. 2) show an example of a set of wheels, where the driving pulley (1) has the number of teeth  $z_1 = 6$ , and the idler wheel  $z_2 = 7$

Two cycloidal wheels, the active wheel (1) and the passive wheel (2) are the main working subassemblies of the machine. These wheels have an internal gearing. The passive wheel in this assembly has a greater number of teeth than the active wheel. The difference in the number of teeth is always  $z_2 - z_1 = 1$ . Figures (Fig. 1, Fig. 2) show an example of a wheel assembly, where the active wheel (1) has the number of teeth  $z_1 = 6$  and the passive wheel  $z_2 = 7$ .

The wheel assembly is placed in the central body (3) and on the sides there are the front console (4) and the rear cover (5).

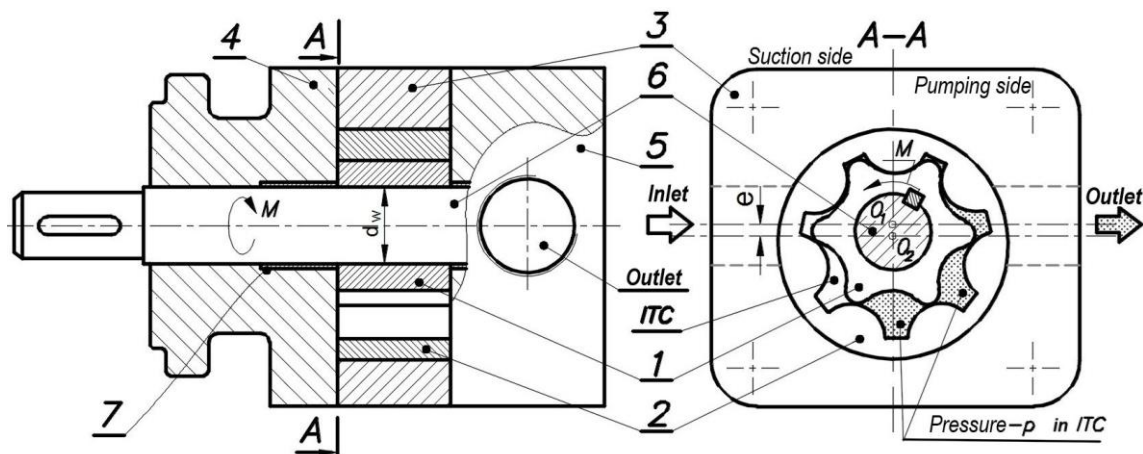


Fig. 1. Design and principle of operation of a hydraulic gerotor machine

Drive and energy are transmitted from the shaft (6) to the active wheel (1). The drive shaft (6) is placed in bearings (7), fixed in the front console (4) and the rear cover (5). Intertooth chambers (ITCs) appear between the wheels after the wheel assembly is installed on the shaft (6) and in the body (3).

The driving torque  $M$  sets the cycloidal wheel assemblies (1) and (2) into rotation. As a result of this motion, the working fluid is transported in the inter-tooth chambers from the inlet hole to the outlet hole. As it rotates, pressure in the pumped fluid increases until the working pressure  $p$  is reached. The vertical symmetry axis of the  $O_1O_2$  wheel assembly divides the hydraulic gerotor machine into two sides, the suction side and the discharge side. The working pressure  $p$  on the discharge side (right, A-A section) acts on the wheel assembly and on components of the body.

Both wheels rotate in the same direction and there is an eccentricity  $e$  between the wheel centres. The active wheel (1) rotates around the centre of the axis  $O_1$ , while the passive wheel (2) rotates around the centre of the axis  $O_2$ .

During operation of a hydraulic machine, the wheel assembly is subjected to mechanical and hydraulic loads. These loads result in a complex state of stress and deformation. Finite element analysis (FEM) was used to determine the stresses.

FEM analysis was used by Gamez-Montero, Castilla, Khamashta and Codina [2]. They proved that maximum stress was found in a pair of teeth moving around the central point of the toothing.

FEM analyses on the strength of epitrochoids working in rotational motion were also carried out by Maiti [3]. Maiti demonstrated that deformations of each tooth have different parameters and allow the flow of the fluid pumped through the machine's inter-tooth canals [3].

The analyzes of flat two-dimensional models were described in [2, 3]. In papers [4, 5, 6], 3D models of cycloidal wheel assemblies were presented. Wheel assemblies made of plastics were analysed and the conclusions from earlier publications were also confirmed [2, 3].

Other work concerned estimation of the working parameters of gerotor machines [7], as well as their geometry [8]. Maiti, Nag and Nagao found that the initial torque depends on the position of the drive shaft [7]. The work [8] shows the unification of geometrical solutions for designing.

Numerical analysis with use of the finite element method enabled determining the behavior of the cycloidal wheel assembly. The steel wheel assembly, loaded with a working pressure  $p = 4$  MPa and a torque  $M = 7.16$  Nm was analysed. These loads were selected for the analysis as in the previous tests the parameters  $p = 4$  MPa and  $M = 7.16$  Nm were used [4, 5, 6].

The method of fixation and loading with pressure  $p$  and torque  $M$  can be seen in Fig. 1 and Fig. 4. The mechanical load with the torque  $M$  was applied to the wall of the keyway in the inner wheel, as shown in Fig. 1 (cross-section A-A).

The hydraulic load of the working pressure  $p$  was applied on the discharge side in the inter-tooth chambers ITC (Fig. 1, cross-section A-A). The pressure  $p$  in the inter-tooth chambers was applied in the same way as in the computational model in Fig. 4.

The method of fixation results also from the operation mode of the machine as in Fig. 1. The active wheel is fixed in the inner hole to simulate fixation of the inner wheel (1) on the shaft (6). The outer wheel (2) is also fixed in the hole of the central body (3), allowing the wheel assembly to rotate around the axis  $O_2$ . This was done in the same way as for the model shown in Fig. 4.

The wheel set was also fixed along the Z axis to reflect the pressing the wheel assembly against the surface of rear cover (5). This fixation and pressure are shown in Fig. 4 as so-called frontal fixation along the Z axis and pressure  $p$  on the wheel face.

Result of this analysis is shown in Fig. 2, where the distribution of stresses and displacements for a loaded set of cycloidal wheels can be observed.

Based on the numerical analysis, the complexity of the stress state in the set of wheels under load was confirmed. This state includes both compressive static loads, as well as fatigue and contact loads.

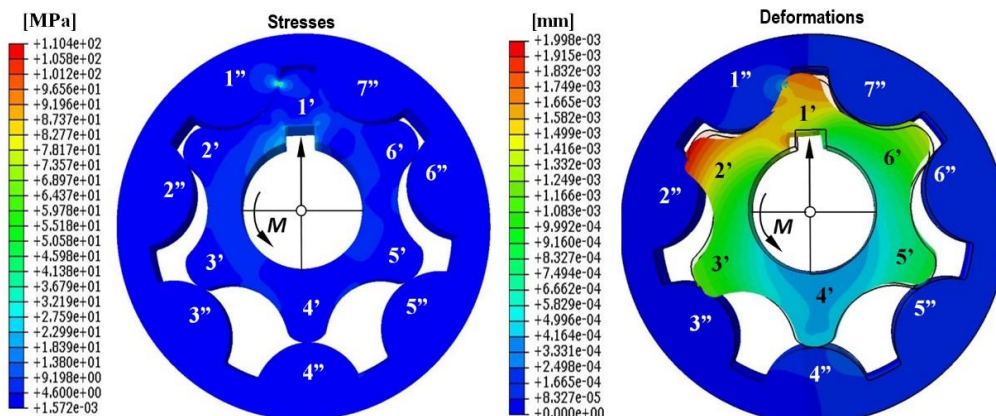


Fig. 2. Distribution of reduced stresses and displacements in a cycloidal wheel assembly

The highest reduced stresses appear in the active wheel at the point of contact of the 1'-1 "tooth pair and in the area of the keyway. The maximum value of these stresses was about 110 MPa.

Working loads also cause displacements in the cycloidal wheel assembly. It can be observed, in Fig. 2, that the greatest displacements were found in the inner wheel for the tips of the 1' and 2' teeth and on the wall of the keyway (red contours). However, these displacements do not have a significant effect on the operation of the hydraulic machine.

The most dangerous displacement takes place in the 4'-4 " tooth pair. The working pressure of fluid in the inter-tooth displacement chambers (ITC) acts on both wheels, causing the 4' tooth to deflect to the left. The 4' tooth in the inner wheel then bends towards the suction side. As a result of this deflection, there is an inter-tooth radial clearance (hr). This causes the machine to leak and its efficiency to drop as a result of leaks.

However, the analysis shows that the displacement of the nodes for tooth 4' is very small - less than 0.0005 mm.

Issues related to designing and operation of hydraulic gerotor machines are realized by the Fluid Power Research Group (FPRG) from the Faculty of Mechanical Engineering at the Wrocław University of Science and Technology ([www.fprg.pwr.wroc.pl](http://www.fprg.pwr.wroc.pl)).

Projects covering technological, designing, operational and visualization aspects are the results [4, 5, 6, 10]. Visualization allowed to define the flow directions and show the cavitation issue [10]. The conclusions from numerical analyses, indicating that higher stresses prevailed in the inner wheel [2, 3, 4, 5, 7], were also confirmed.

It is therefore necessary to introduce changes aimed at increasing the load capacity of cycloidal wheels. To achieve this goal, however, it is necessary to introduce changes to the design of the wheel assembly, but also in a principle of operation of the hydraulic gerotor machine.

In each of the solutions, known to the author, drive in the wheel assembly is transmitted from the inner wheel to the outer wheel.

The solution used so far has several disadvantages. These disadvantages were proved both by numerical analyzes [2, 3, 4, 5] and tests [6]. These disadvantages can be summarized in several points and they are as follows:

- significant stress in the inner wheel,
- high concentration of stress in the contact places of wheels teeth, especially in the 1'-1 " tooth pair,
- high stress in the area of the hole in the active (inner) wheel, caused by transmission of the drive from the drive shaft to the active wheel,
- small diameter of the driving shaft  $d$ , limited by the diameter of the tooth base in the active wheel,
- asymmetric stress distribution in the wheel assembly.

All these disadvantages limit the range of the operational parameters with which hydraulic gerotor machines.

It should also be added that the smaller size of the inner active wheel causes that stress relaxation in this wheel is difficult, and thus stress concentrations appear in it.

It can be observed that there is a need to change the design concept for hydraulic gerotor machines. New design of a hydraulic gerotor machine should be work objective. This solution should ensure higher operational parameters, without increasing dimensions and weight of the machine.

## 2. Materials and Methods

### 2.1. New solution

New solution was developed by changing the role of both cycloidal wheels, so that the outer wheel is now the driving wheel, and the inner wheel is now the driven wheel.

The solution was described in the patent application (Gerotor hydraulic machine. Application No. P. 416532. Case mark 451-9/16).

The hydraulic gerotor machine according to the new concept, in which the role of the wheels was changed is shown in Fig. 3. In the system shown in Fig. 3, the drive is first transmitted to the outer wheel (2), while the inner wheel (1) now acts as a passive (driven) wheel.



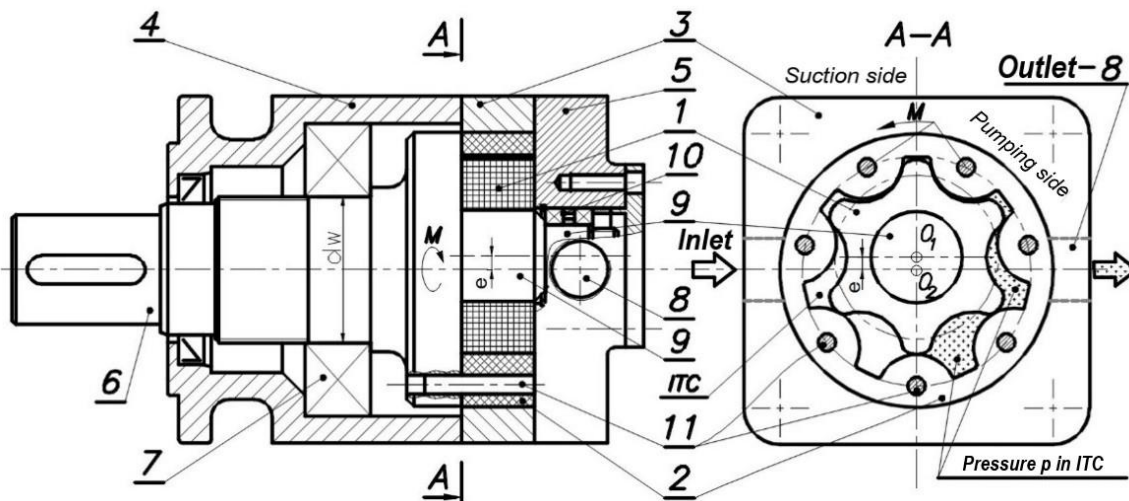


Fig. 3. Scheme of a hydraulic gerotor machine according to the new concept

The inner (1) and outer (2) wheels are still the main working components of the hydraulic gerotor machine (Fig. 3).

A set of cycloidal wheels (1) and (2) is located in the central body of the hydraulic machine (3). The hydraulic machine body assembly consists of a central body (3), a front console (4) and a rear cover (5). Pins (11) connect outer wheel (2) to driving shaft (6). Front console (4) contains bearing assembly (7) for the driving shaft (6). The outlet hole for pumped liquid (8) is located in the rear cover (5).

Fig. 3 shows that the inner wheel (1) is mounted on the second shaft (9). The shaft (9) is supported by a bearing unit (10), placed in the hole of the rear cover (5).

The connection between the inner wheel (1) and the shaft (9) is close fit.

In the solution shown in Fig. 3, the cycloidal wheels (1) and (2) are still in contact with each other by their inter-tooth contacts, as in the previous solution (Fig. 1). It can therefore be said that:

- the outer wheel (2) rotates with the drive shaft (6) in bearings (7) around its axis  $O_1$ ,
- the inner wheel (1) rotates with the shaft (9) in bearings (10) around its axis  $O_2$ .

The eccentricity  $e$  is both between the wheel axes (1) and (2) and between the shaft axes (6) and (9) on which these wheels are embedded. The outer wheel (2) is connected to the drive shaft (6) using the special pins (11).

These pins (11) are used to transmit power and energy from the shaft (6) to the outer wheel (2). The A-A section (Fig. 3) shows that the number of pins corresponds to the number of teeth in the outer wheel (2). The number of pins equal to the number of teeth in the outer wheel, ensures an even distribution of the load in this wheel. In the example shown in this description, there are seven pins (Fig. 3).

Energy of torque  $M$  is transmitted from the driving shaft (6) to the outer wheel (2) via pins (11). The outer wheel (2), which now operates as an active wheel, sets the inner wheel (1), mounted on the shaft (9), into rotation.

The liquid flows from the left side (see section A-A in Fig. 3) to the inter-tooth chambers and is forced by the rotation of the wheels to the outlet (8) on the right side (A-A). The mechanical energy is then converted into hydraulic pressure in the inter-tooth chambers.

## 2.2 Computational model

A geometric model of the cycloidal wheel assembly was developed using the construction diagram of the gerotor pump shown in Fig. 1 and 3. The model is shown in Fig. 4. The toothing profiles of both wheels were determined on the basis of the literature [9].

During operation, the wheel assembly is subjected to hydraulic and mechanical loads. The hydraulic load of the model results from the pressure  $p$  of the working medium, while the mechanical load results from the application of the driving torque  $M$ .

The working pressure  $p$  acts in the inter-tooth chambers and on the front surfaces of both wheels. The wheel assembly remains in equilibrium because the torque  $M$  applied to the outer wheel is equal to the torque induced by the pressure  $p$ . Mechanical load by torque  $M$  is transferred to the larger outer wheel, what can be observed in the model.

The torque  $M$  was applied to seven holes made in the teeth of the outer wheel. In this way the torque  $M$  was distributed evenly between the seven teeth of the outer wheel. The model should be restraint, and the method of restraining also results from the principle of operation of gerotor pump.

Fig. 3 shows that the inner wheel is mounted on the shaft and can only be rotated around the axis  $O_1Z$ . In the model shown in Fig. 4, this wheel is radially fixed on a shaft with a diameter  $d_1 = 25$  mm and rotates around the axis  $O_1Z$ .

The outer wheel in Fig. 3 can rotate inside the body around the  $O_2Z$  axis.

In the model shown in Fig. 4, this wheel is restraint radially on a diameter  $d_2 = 75$  mm, but it can rotate around the axis  $O_2Z$ . The system is also loaded with the pressure  $p$  of the working medium in the gap between the wheel assembly and the body components. The wheel assembly is thereby pressed against the body by a pressure  $p$  exerted on the wheel face surfaces.

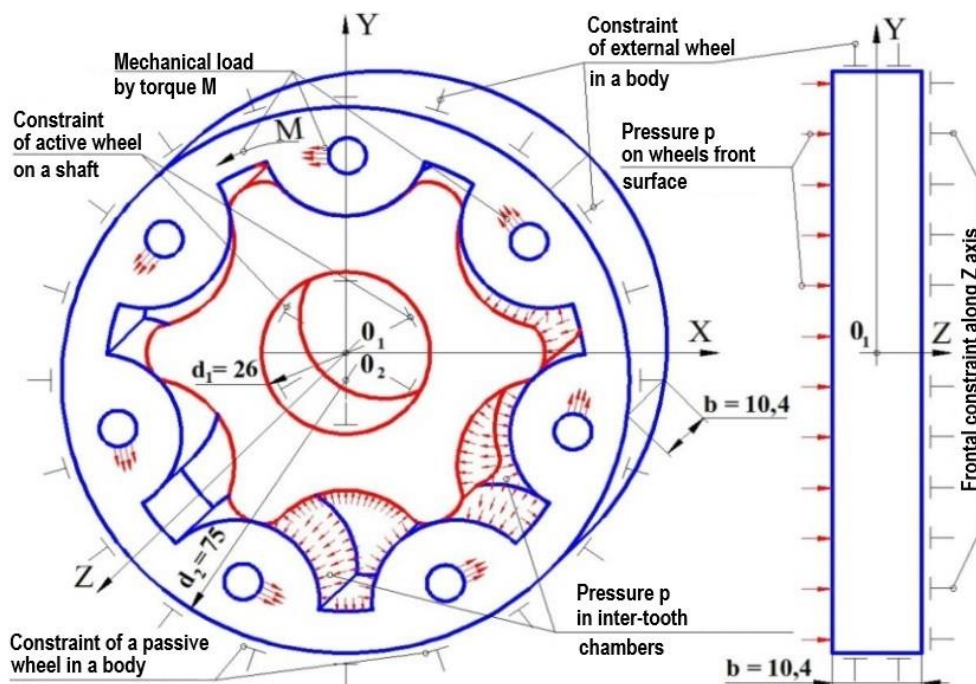


**Fig. 4.** Computational model of wheel assembly for a new method of drive transmission – a diagram of loads and restraints

Therefore, in the model shown in Fig. 4, the front surface of the wheel assembly is loaded with pressure  $p$ , while the opposite face is fixed frontally along the  $Z$  axis.

The numerical model of the cycloidal wheel assembly was created using the ABAQUS version 6.14-2 system. The license for this program, number 05UWROCLAW, was made available by the Wrocławskie Centrum Sieciowo-Superkomputerowe at the Wrocław University of Technology. HEXA-type cubic elements shown in Fig. 5a were used to develop the finite element mesh shown in Fig. 5b. These are typical elements for creating solid models [11]. The use of HEXA-type elements made it possible to create 3D model of the wheel assembly. The HEXA element is cube-shaped with 8 nodes. The number of nodes indicates that it is a first order element. Each node of the HEXA element can be moved in relation to  $X$  axis,  $Y$  axis and  $Z$  axis [11].

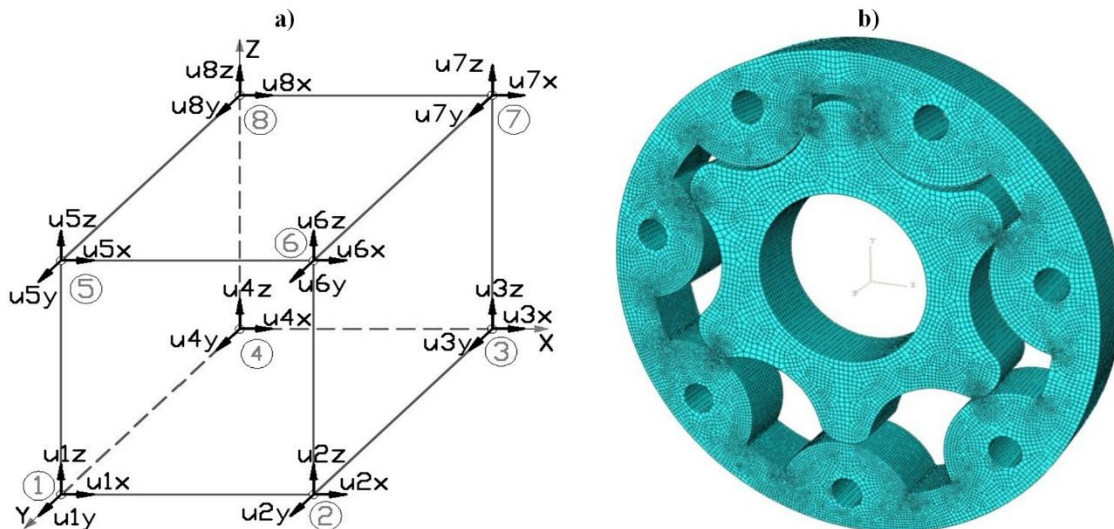


**Fig. 5.** HEXA type element and mesh of cycloidal wheel assembly created of HEXA type finite elements

Triangular and quadrilateral elements were used to build two-dimensional meshes of 2D cycloidal wheels [2, 3]. They were both first order and second order elements.

2D models gave the results close to the real ones. Creating 3D model allows to increase calculations accuracy, due to the better correlation of the 3D model with real conditions, as the wheel assembly was a 3D structure. Total load and restraints cannot be included in 2D models. Only in the 3D model it is possible to include pressure to the front wheels surface and the frontal restraint along the Z axis (see Fig. 4). 3D model takes into account total load to the wheel assembly. Such a model allows to estimate the axial clearance (in direction of the Z axis). This was not possible in the case of 2D models. Even if axial clearance will have a slight share in the displacement, this value should be taken into account in the analysis of the hydraulic operation of the gerotor machine. For these reasons, 3D model of the cycloid wheel assembly was created.

The finite element mesh for the wheel assembly was created of approximately 500,000 HEXA elements. The elements formed the outline of the wheel assembly in the XY plane. Fifteen layers of HEXA elements were created to model the thickness of the wheel assembly. These layers were spaced approximately every 0.7 mm along the OZ axis until obtaining the proper thickness of the wheel assembly  $b = 10.4$  mm (Fig. 4).

Mesh densification was entered at the location of predicted stress concentration, see Fig. 5b. Points of densification are the teeth contacts of the cooperating wheels at the input side (left side of the model in Fig. 5b). Lower densification was in the corners at the base of the teeth of the outer wheel.

Previous tests show that the stresses in the tooth are of a contact nature [2, 3, 12, 13]. The HEXA element is also very good for modelling just such contacts [12, 13].

The ABAQUS system also enabled to model the contact of cooperating surfaces using a special algorithm for this system. The contact of the teeth of the wheels was assumed at the low pressure zone (left side of Fig. 4 and Fig. 5b).

The coefficient of friction  $\mu$  for the contact was selected for the steel-steel contact and the most unfavorable case was adopted, i.e. for dry friction, which is  $\mu = 0.1$ .

The numerical model enabled determining the stresses and strains for the wheels assembly with high accuracy. Discretization errors did not exceed 0.02% for deformations and about 1.3% for stresses. These errors were estimated using the relationships provided in the literature [11].

### Test program and selection of parameters for numerical analysis

At the beginning, the wheel assembly model operating under working pressure  $p = 4$  MPa and torque  $M = 7.16$  Nm was analyzed. The initial parameters pressure  $p = 4$  MPa and torque  $M = 7.16$  Nm were taken basing on previous publications [4, 5].

Aim of this analysis was to find design solutions that would allow to exceed this limit. For this reason, the parameters  $p = 4$  MPa and  $M = 7.16$  Nm were taken as the starting values, as the lowest.

In the next stages, working pressure  $p$  and torque  $M$  were increased. According to the test program, the model of wheel assembly was analyzed for pressures  $p = 4, 8, 12, 16, 20$  and  $24$  MPa and with a proportionally higher torque  $M$ .

The load parameters are presented in Table 1.

**Table 1.** Computational parameters

Working pressure $p$ [MPa]	Torque $M$ [Nm]
4	7.16
8	14.32
12	21.48
16	28.66
20	35.82
24	42.96

Cycloidal wheels are usually made of high-grade steel. The steel was 18HCrMo4 steel (former symbol 18HGM) intended for carburizing. Strength parameters of 18HCrMo4 steel are given in Table 2.

**Table 2.** Technical parameters of 18CrMo4 steel 18CrMo4 (18HGM)

Item	Parameter	Symbol	Value
1.	Yield point	$Re$	830 MPa
2.	Young's modulus	$E$	210000 MPa
3.	Steel/steel friction coefficient	$\mu$	0.1
4.	Safety factor [14]	$x$	$1.4 \div 1.6$

To analyze the solution, the permissible stress and displacements for cycloidal wheels assembly should be determined.

The permissible displacements depends on the radial clearance  $hr$ . The  $hr_{DOP}$  can be determined on the basis of the literature [9]. It was assumed that the permissible  $hr_{DOP} = 0.1$  mm and the  $hr$  clearance cannot exceed the  $hr_{DOP}$ .

The permissible stress should be determined using the  $Re$  for 18CrMo4 steel and dividing it by the safety factor  $x$  for gears [14]. When the safety factor is  $x = 1.5$ , the allowable stress is  $\sigma_{DOP} = 550$  MPa.

The numerical analysis was continued until one of the above permissible values ( $hr_{DOP} = 0.1$  mm,  $\sigma_{DOP} = 550$  MPa) was exceeded.

### 3. Results of numerical analysis

Fig. 6 shows distributions of stresses and displacements for wheel assembly, when direction of drive transmission is changed. These distributions differ from those seen in the previous solutions [2, 4, 5] and in Fig. 2.

The maximum stress appears for tooth 1', the same as in the traditional solution shown in Fig. 2. However, there are also the following differences:

- the maximum stress is located on the pressing side in the tooth pair 1'-7'', not on the suction side, as in the traditional solution (in the 1'-1'' tooth pair),
- the maximum stress (in the contact of the 1'-7'' pair) is 72 MPa and is about 35% lower than in the traditional solution (for the 1'-1'' pair in Fig. 2).



The change in position of maximum stress is the result of a change in the direction of energy transmission.

In the new solution, the drive is transmitted to the outer wheel via pins (No. 11 in Fig. 3). In this case, the groove is omitted and therefore there is no groove in the hole in the inner wheel. The connection between the shaft and the inner wheel was made fit ( $\varnothing 25H7/p6$ ). For this reason, the hole in the inner wheel was strained, but the stress is lower than the stress in the contact of tooth pair 1'-7''.

The greatest displacement in the described solution is now in the outer wheel. In the traditional solutions described in the literature, the inner wheel was significantly more strained [2, 4, 5] and more deformed (Fig. 2). In the new solution, the opposite is true. However, it can be seen from Fig. 6 that the maximum displacement (red) should not have a significant impact on operation of the wheel assembly.

Deformation most disadvantageous for the machine operation was found for the 4'-4'' tooth pair, due to bending of this pair of teeth towards the suction zone, the same as for the previous solutions.

However, it should be noted that the displacement as a radial clearance  $h_r$  is much lower than the permissible value  $h_{rDOP} = 0.1$  mm. This displacement is low for both wheel assembly designs.

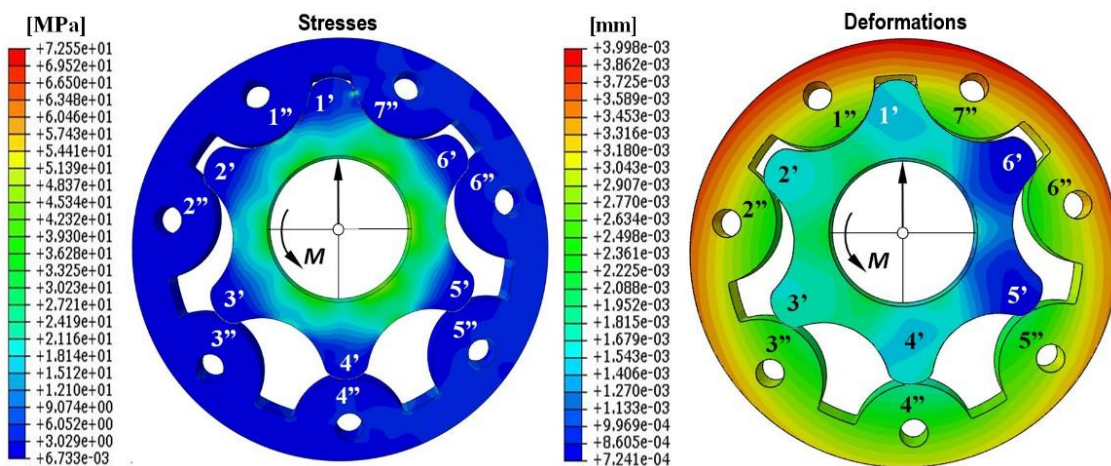


Fig. 6. Distribution of reduced stresses and deformations in a cycloidal wheel assembly according to the new solution

Fig. 7 and Table 3 present the result of the analysis in a comprehensive manner for both methods of drive transmission, which are shown in Fig. 1, 2, 3 and 6.

By analyzing Fig. 7 and data from Table 3, it can be observed that the wheel assembly according to the new solution (Fig. 3 and Fig. 6) shows lower stress in the 1'-1'' tooth pair than the traditional solution (Fig. 1, 2). However, the traditional solution shows a lower radial clearance  $h_r$ . Therefore, the new solution is better in terms of stresses, while the traditional one is better in terms of the radial clearance  $h_r$ .

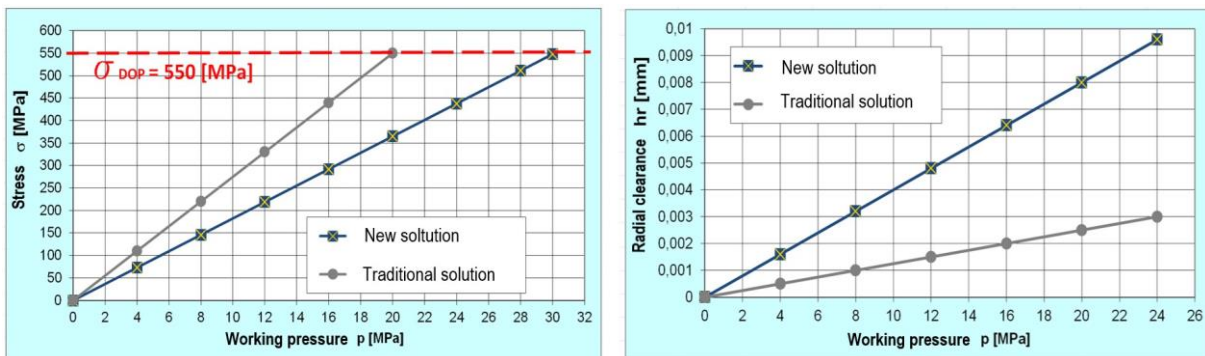


Fig. 7. Change of reduced stresses and deformations depending on the working pressure  $p$  for two types of cycloidal wheels

As the load (pressure  $p$ ) increases, strain in the wheel assembly increases and the increase is linear (Fig. 7).

In the new solution, the stress is lower. According to the author, this may be due to a more even distribution of the force producing torque  $M$ . The force producing torque  $M$  is evenly distributed over the seven pins. This factor reduces the stresses in wheel assembly made according to the new solution, as shown in Fig. 3.

**Table 3.** Strength analysis with the use of FEM for the cycloidal wheel assembly

Working pressure $p$ [MPa]	Reduced stress $\sigma$ [MPa]		Radial clearance $h_r$ [mm]	
	Traditional solution [Fig. 2]	New solution [Fig. 6]	Traditional solution [Fig. 2]	New solution [Fig. 6]
4	110	73	0.0005	0.0016
8	220	146	0.001	0.0032
12	330	219	0.0015	0.0048
16	440	292	0.002	0.0064
20	550	365	0.0025	0.008
24		438		0.0096
28		511		0.0112
30		548		0.0192

When analyzing Fig. 7 and Table 3, it can be concluded that gerotor machine with the new type of drive, enables obtaining the higher working pressure  $p$  than with a traditional drive transmission system.

Attention should also be paid to strength criterion. The analysis shows that for both designs (Fig. 2 and 6), a possible failure can occur as a result of destruction of the wheel assembly by increased stresses. This destruction can happen much faster before the increase in radial clearance  $h_r$  causes loss of tightness and thus a decrease in volumetric efficiency for hydraulic gerotor machine.

#### 4. Conclusions

Presented solution shows the method for increase the load limit for a cycloidal wheel assembly and a hydraulic gerotor machine.

In literature [9] describing the behaviour of wheel assembly under load, it was assumed that all pairs of teeth on the passive side are in contact [9]. An additional assumption was that the load is transferred evenly. According to this assumption, the forces acting in pairs of teeth in contact with each other are equal [9]. The numerical analysis does not confirm these assumptions.

However, the analysis confirms the need for searching a new design of hydraulic gerotor machines.

The result of analysis indicates that the hydraulic gerotor machine, designed according to the new concept, can operate with a higher working pressure  $p$ . Working loads for the new unit can be about 35% higher than for a wheel assembly using a traditional transmission method (Fig. 1 and 2).

The possibility of applying new concepts in the design of gerotor machines should be considered both from the deformation and allowable stresses point of view.

Stresses in the wheels should not exceed the stress limits ( $\sigma_{DOP} = 550$  MPa), causing possible damage to the wheel assembly. At the same time, deformation of teeth and the resulting inter-tooth clearance  $h_r$  should not exceed the adopted limit. Exceeding this value will result in loss of tightness, leakage and reduced machine efficiency. Based on literature data, it was assumed that the maximum clearance  $h_r$  should not exceed the permissible clearance of  $h_{rDOP} = 0.1$  mm [9].

Regarding the stress, the new solution of the wheel assembly can operate up to the  $p = 30$  MPa of working pressure, while the traditional one can operate up to the pressure of  $p = 20$  MPa. Therefore, the new solution is more advantageous in this aspect.

However, regarding the inter-tooth clearance  $h_r$ , the traditional solution has better parameters. For both solutions the clearance  $h_r$  is much lower than the permissible clearance, established as  $h_{rDOP} = 0.1$  mm. When analysing the diagram in Fig. 7 for the clearance  $h_r$ , it is clear that it does not exceed  $h_r = 0.012$  mm.

Therefore, the deformations are kept within the limits and there is no threat of unsealing the gerotor machine for both types of drive transmission. It can be observed that the stress level is more important here. For both solutions, an increase in stress will destroy the wheel assembly sooner than a decrease in efficiency as a result of leakage.

When choosing a solution, the stress criterion should be taken into account rather than the criterion of deformations. Therefore, it becomes justified to introduce a new type of drive transmission for hydraulic gerotor machines. The new type of drive lowers the stress in the wheel assembly.

Reducing the stress demonstrates the importance of introducing a new method of transmitting the drive to the cycloidal wheel assembly. The analysis shows that the new solution can operate up to the working pressure of  $p = 30$  MPa.

However, there will also be other factors that can reduce the assembly strength. These factors include manufacturing and assembly inaccuracies, fatigue strength, temperature-dependent dimensional changes and other operating conditions.

All these factors are difficult to predict and therefore also difficult to include in numerical analysis. However, an attempt should be made to reduce the final load capacity range for the analyzed wheel assembly.

Based on the analysis the following can be observed:

- A wheel assembly with a changed direction of drive transmission can theoretically work up to a pressure of about  $p \leq 30$  MPa. However, after taking into account the factors reducing the strength, the load capacity range should also be reduced to the working pressure  $p \leq 25$  MPa.

According to the author, the presented solution can be used for hydraulic systems with the increased working pressure  $p$ .

The above analysis does not exhaust the subject and further studies on design modifications can be continued.

## References

- [1] Lewandowski K.: A change the structural of railway loading stations for containerization. LOGISTYKA No. 4/2012, ISSN 1231-5478, pages 483-494
- [2] Gamez-Montero P. J., Castilla R., Khamashta M., and Codina E.: Contact problems of a trochoidal gear pump. International Journal of Mechanical Science. 2006, (12)
- [3] Maiti R.: Active Contact Stresses at Epitrochoid Generated ROTOR-STATOR set of Fixed Axis or Equivalent system 'ROPIMA' type Hydrostatic units, ASME Journal of Engineering for Industry, 113(4):465-473.2. 1991
- [4] Biernacki K., Stryczek J.: Analysis of stress and deformation in plastic gears used in gerotor pumps. The Journal of Strain Analysis for Engineering Design, October 2010, vo.45, Issue 7, pages 465-479
- [5] Stryczek J., Bednarczyk S., Biernacki K.: Strength analysis of the polyoxymethylene cycloidal gears of the gerotor pump. ARCHIVES OF CIVIL AND MECHANICAL ENGINEERING (2014). Vol. 14, No. 4. Pages 647 – 660. <http://dx.doi.org/10.1016/j.acme.2013.12.005>
- [6] Stryczek J., Bednarczyk S., Biernacki K.: Gerotor pump with POM gears: Design, production technology, research. ARCHIVES OF CIVIL AND MECHANICAL ENGINEERING, 2014, Vol. 14, No. 3. Pages 391 – 397. <http://dx.doi.org/10.1016/j.acme.2013.12.008>
- [7] Maiti R., Nagao M.: Prediction of Starting Torque Characteristics of Epitrochoid Generated Orbital Rotary Piston Hydraulic Motors, JSME International Journal of Mechanical Systems, Machine Elements and Manufacturing, C 42(2): pages 416-426. 1999
- [8] Nag A., Maiti R.: Unification of Epitrochoid origin profile design approaches for external lobed Star member used in hydrostatic and gear units. Institution of Mechanical Engineers Part-C: Journal of Mechanical Engineering Science, UK. May 24, 2012, 227(2), pages 299-310. DOI: 10.1177/0954406212448365
- [9] Stryczek J.: Cycloidal gears in design of gear pumps and motors. Habilitation Dissertation. Scientific Papers of the Institute of Machine Design and Operation of Wroclaw University of Technology. Series: Monographs nr 15. Wroclaw 1991

- [10] Antoniak P., Stryczek J.: Archives of Civil and Mechanical Engineering Volume 18, Issue 4, September 2018, Pages 1103-1115. <https://doi.org/10.1016/j.acme.2018.03.001>
- [11] Rusiński E., Czmochoowski J., Smolnicki T.: Advanced finite element method in the load-bearing structures Publishing House of Wrocław University of Technology. Wrocław 2000
- [12] Smolnicki T., Harnatkiewicz P., Stańco M.: Degradation of a geared bearing of a stacker. Archives of Civil and Mechanical Engineering. 2010, vol. 10, nr 2, p. 131-139
- [13] Smolnicki T.: Large - size bearings in opencast mining machines. Design and selection of bulk material handling equipment and systems: mining, mineral processing, port, plant and excavation engineering. Vol. 1 / ed. by Jayanta Bhattacharya. Kolkata: Wide Publishing, 2012, pages 105-130
- [14] Banaszek J., Jonak J.: Podstawy konstrukcji maszyn. Wprowadzenie do projektowania przekładni zębatych i doboru sprzęgieł mechanicznych. Politechnika Lubelska. Wydawnictwo Uczelniane 2008, str. 26